



Ewa Olejnik*, Andrzej Janas, Andrzej Kolbus, Beata Grabowska

AGH University of Science and Technology, Faculty of Foundry Engineering, ul. Reymonta 23, 31-266 Krakow, Poland

* Corresponding author. E-mail: eolejnik@agh.edu.pl

Otrzymano (Received) 27.02.2011

COMPOSITE LAYERS FABRICATED BY IN SITU TECHNIQUE IN IRON CASTINGS

The paper presents the results of studies on the development of 3 to 6 x 10⁻³ m thick composite layers in iron castings. The said layers are formed by an SHS reaction that occurs between the substrates, i.e. titanium and carbon, introduced into the mould. outcome is the synthesis of TiC carbides in a liquid alloy, where the hardness of these layers is 1950 MHV and the size ranges from 2 to 10 x 10⁻⁶ m. Within the layer, locally coagulated clusters are formed. The stoichiometric mixture of titanium and carbon powders introduced to the mould, provokes changes in the alloy solidification conditions. This was confirmed by a DTA analysis, the results of which have indicated a change in the chemical composition of the alloy and local temperature rise in the reaction zone, amounting to 85 K respective of the remaining part of the casting.

Keywords: composite layers, in situ composite, SHS reaction, synthesis TiC, iron casting

WARSTWY KOMPOZYTOWE OTRZYMYWANE IN SITU W ODLEWACH Z ŻELIWA

Przedstawiono wyniki badań dotyczące otrzymywania in situ warstw kompozytowych w odlewach z żeliwa. Powstają one w następstwie reakcji SHS (Self-Propagating High-Temperature Synthesis) zachodzącej pomiędzy wprowadzonymi do formy substratami, tj. tytanem i węglem. Inicjatorem reakcji jest zalewany do formy ciekły metal o temperaturze 1652 K. Wytworzone w wyniku burzliwej reakcji węgliki ulegają rozproszeniu w ciekłym metalu, tworząc po procesie krystalizacji osnowy warstwę kompozytową o grubości od 3 do 6 x 10⁻³ m. Wielkość uzyskanych faz ceramicznych o kształcie zbliżonym do owalnego wynosi od 2 do 10 x 10⁻⁶ m. Tworzą one w obrębie warstwy lokalnie zwarte i skoagulowane formy, a ich maksymalna twardość wynosi 1950 MHV.

Otrzymane krzywe TDA stopu bazowego oraz stopu zawierającego mieszaninę substratów reakcji SHS na dnie formy wskazują na różnice w procesie krystalizacji obu tych materiałów. Dotyczy to głównie krystalizacji stopu zawierającego substraty reakcji SHS, w którym obserwuje się brak efektu cieplnego wywołanego krystalizacją austenitu pierwotnego. Efekt ten widoczny jest w stopie bazowym. Wynik taki wskazuje na zmianę składu stopu wywołaną wprowadzonymi do formy proszkami, tj. tytanem i węglem. Ponadto silnie egzotermiczna reakcja syntezy węglików prowadzi do wzrostu temperatury w strefie reakcyjnej o 85 K.

Słowa kluczowe: warstwy kompozytowe, kompozyty in situ, reakcja SHS, synteza TiC, żeliwo

INTRODUCTION

Ferro-alloys of increased hardness represent the largest group of materials used in the manufacture of structural components resistant to abrasive wear. Among them, the most popular continue to be various grades of cast steel, mainly martensitic, and austenitic with manganese and chromium, and to a lesser extent cast irons, mainly white martensitic, and various chromium-alloyed grades. Other commonly used materials are abrasion resistant sinters [1, 2], cermets [3, 4], bi-metals [5, 6], and stellites [7]. All these materials are fabricated by using, among others, techniques such as: casting [8, 9], powder metallurgy [10], and surface engineering, including the increasingly popular LISHS (Laser Ignited Self-Propagating High-Temperature Synthesis) [11, 12] and LPPS (Low Pressure Plasma Spraying) processes [13].

Generally, abrasive wear resistant materials are divided into bulk-hardened or locally hardened materials. Bulk-hardened materials have similar properties along their entire cross-section, making them either very hard and brittle, or soft and plastic. In the case of parts locally hardened or having a layer structure, it is possible to obtain a favourable correlation between the very hard working surface and tough core.

One of the possible ways to obtain hard composite layers in castings is through the use of SHS (Self-Propagating High-Temperature Synthesis) [14]. It allows the attainment of hard ceramic phases in a reaction that occurs between the reactive substrates placed in the mould cavity and liquid alloy [15, 16]. As a result of this process, carbides undergo "in situ" synthesis in the surface layer of the casting.

EXPERIMENTAL PROCEDURE

Table 1 shows the chemical composition of the base alloy used in the tests.

TABLE 1. Chemical composition of base alloy
TABELA 1. Skład chemiczny stopu bazowego

Materials	Chemical compositions, mass %					
	C	Si	Mn	P	S	Cr
Base metal	3.64	1.57	0.63	0.05	0.08	0.012

A composition of substrates necessary for the synthesis of titanium carbide was mixed in an atomic ratio corresponding to the TiC carbide-forming reaction. To successfully perform this task, the following commercial products were used: titanium powder of 99.98% purity (Aldrich) and 44 μm granulation, and graphite of 99.99% purity and 30 μm granulation. Then the powders were put together in the proper ratio and mixed for 24 hours. Two Y-shaped moulds were made of molochite by using sodium silicate mixed in a ratio of 1:10 and then were blown with CO_2 ; the corresponding schematic diagram is shown in Figure 1. As the next step, at the bottom of one of the moulds, a mixture of 2×10^{-2} kg of titanium and carbon powders was compacted, while the second mould without the SHS reaction substrates was used for casting the base alloy. The thus prepared moulds were dried at 773 K for 10 min, and then were placed in a Balzers type vacuum chamber furnace.

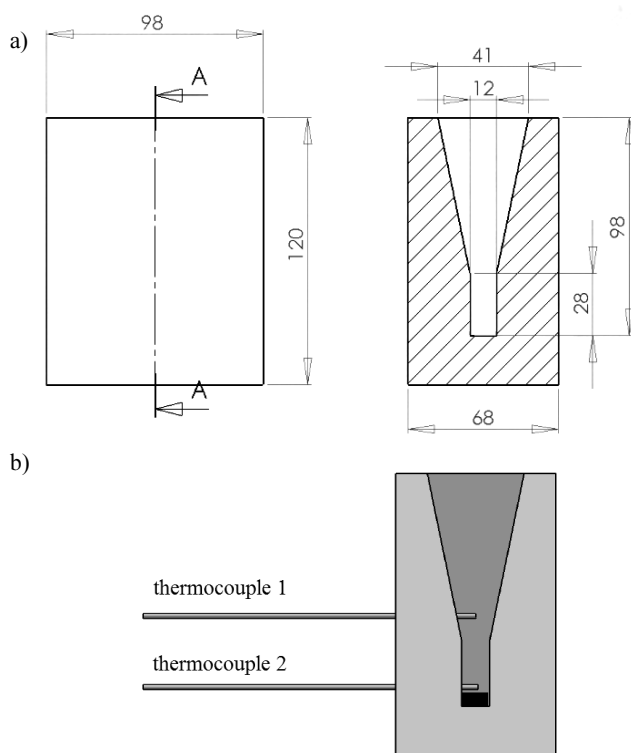


Fig. 1. Schematic diagram showing longitudinal mould section and places where thermocouples were mounted

Rys. 1. Schemat ilustrujący przekrój wzdłużny formy oraz miejsca zamocowania termoelementów

To conduct thermal analysis of the alloy solidification process, two Pt10Rh-Pt (S type) thermocouples were mounted in the mould. Thermocouple 1 was placed in the bottom part of the casting body, while thermocouple 2 was placed in the riser (Fig. 1), observing a distance from the mould bottom of 3×10^{-3} m and 2.5×10^{-2} m, respectively. A cast iron charge of a composition corresponding to the composition stated in Table 1 was introduced into the crucible, and the melting process was carried out under a protective argon atmosphere. The resulting castings were cut into pieces, taking samples from the casting body with a layer of the composite material and from the riser.

Metallographic examinations were carried out using scanning electron microscopy (SEM). The chemicals were measured by energy dispersive spectroscopy (EDS). X-ray diffraction (XRD) analysis with monochromatized $\text{Cu K}\alpha$ radiation ($\lambda = 1.5418 \text{ \AA}$) at a voltage of 30 kV and 25 mA intensity was also performed. The microhardness (MHV) was measured with a Vickers microhardness tester under a load of 0.1 kg during the time of 15 seconds.

RESULTS

Figure 2 shows the phase analysis of the samples taken from the casting body and riser. The main structural constituents present in both test materials are ferrite (α). In the sample taken from the casting body, a second phase obtained by SHS, i.e. titanium carbide, appears.

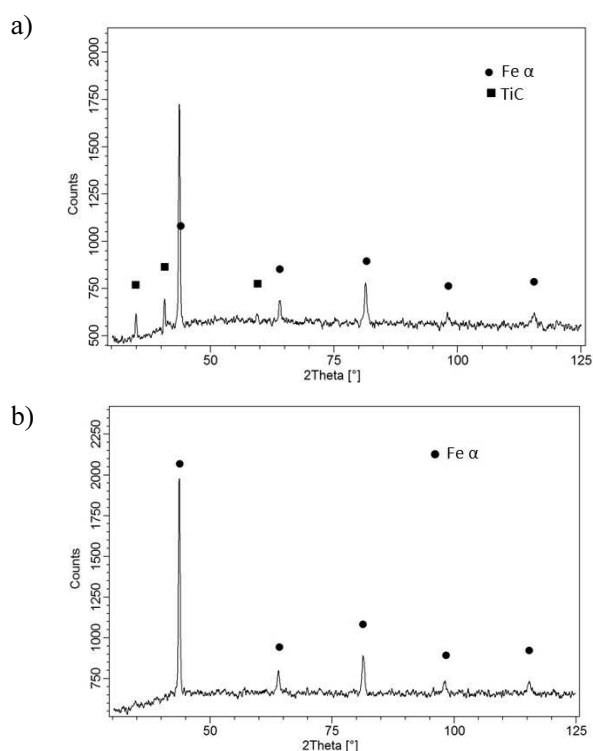


Fig. 2. X-ray diffraction pattern of sample taken from casting body (a) and riser (b)

Rys. 2. Dyfrakcja rentgenowska materiału pochodzącego z trzonu odlewu (a) i nadlewu (b)

Figures 3 to 5 show the examples of BSE (back-scattered electrons) images of the composite layer produced in the iron casting. The layer (grey colour) shown in Figure 3 was formed in the region of the casting surface, and its thickness varied from 3 to 6×10^{-3} m.

The BSE images disclosed in Figure 4 show a transition zone between the composite layer and casting core. The TiC carbides (gray colour) visible in this zone are distributed in the cast iron matrix

with flake graphite (Fig. 4). The size of the TiC carbides obtained by synthesis is in the range of 2 to 10×10^{-6} m, and they are of a nearly oval shape (Fig. 5a). They form clusters of locally coagulated crystals, whose maximum hardness is 1950 MHV. Figure 5b shows the image of the composite layer microstructure with a marked area where TiC crystals have been subjected to X-ray microanalysis, the results of which are given in Table 2.

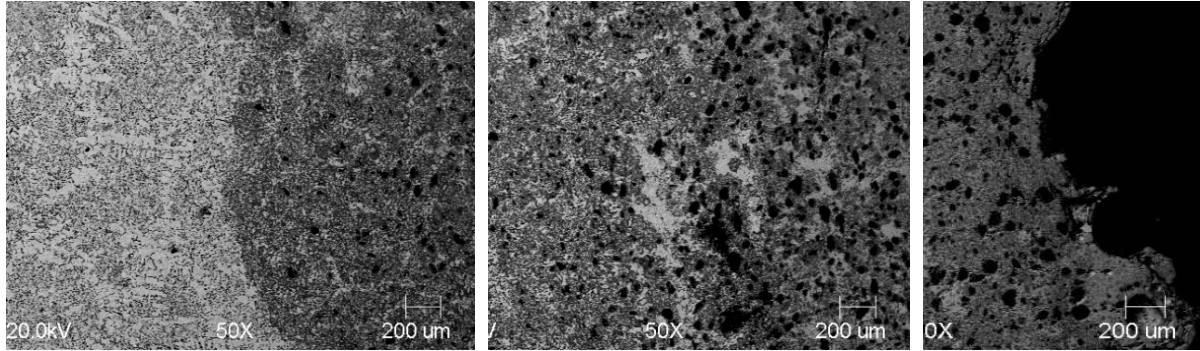


Fig. 3. SEM-BSE micrographs (widescreen) of composite layer produced in cast iron

Rys. 3. Obrazy SEM-BSE warstwy kompozytowej otrzymanej w żeliwie (obraz panoramiczny)

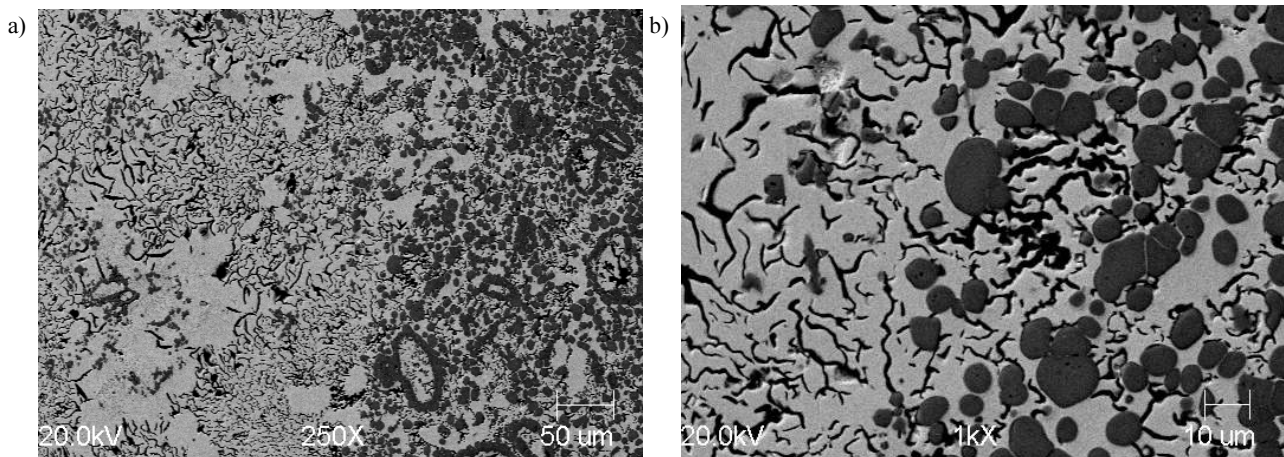


Fig. 4. SEM-BSE image of transition zone between the composite layer and grey iron casting core

Rys. 4. Obraz SEM-BSE strefy przejściowej pomiędzy warstwą kompozytową a rdzeniem odlewu z żeliwa szarego

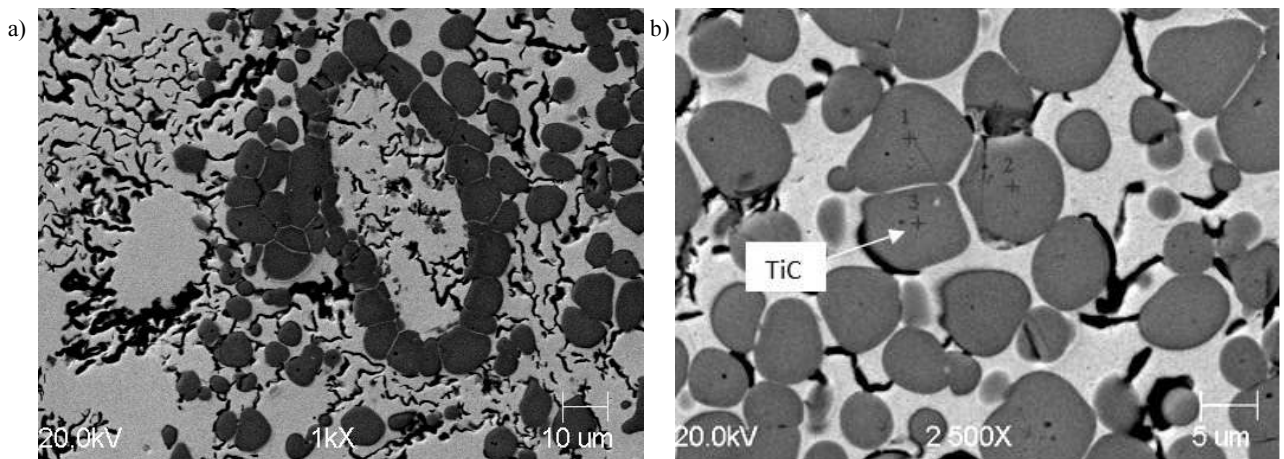


Fig. 5. SEM-BSE image of composite layer with marked points of X-ray microanalysis

Rys. 5. Obraz SEM-BSE strefy kompozytowej wraz z zaznaczonym obszarem mikroanalizy rentgenowskiej

The X-ray microanalysis of points 1-3 (from Fig. 5b) in Table 2 shows the presence of Ti, C and Fe.

TABLE 2. Chemical composition of carbide observed in surface composite layer, measured using EDS

TABELA 2. Skład chemiczny węglików tytanu obserwowany w warstwie kompozytywnej, mierzony przy użyciu EDS

Chemical composition, at.%			
Phase (Point)	Ti	C	Fe
TiC (1)	38.3	61.4	0.3
TiC (2)	35.2	64.6	0.2
TiC (3)	36.8	63.0	0.2

Figure 6a, b shows the cooling curves of the base alloy and their first derivatives plotted for the casting body (a) and riser (b). The solidification of the alloy in the riser recorded by thermocouple 1 ranges in a mode typical of hypoeutectic cast iron. The derivative curve for this alloy shows the four main thermal effects associated with the crystallisation of austenite - ABC points, of graphite and cementite eutectic - DEFG points, and with the transformation of austenite into ferrite - HIJ points and into pearlite - J'KL points. In the case of the second curve (b) recorded in the casting body by thermocouple 2, only thermal effects associated with the austenite transformations (HIJ and J'KL points) are well visible.

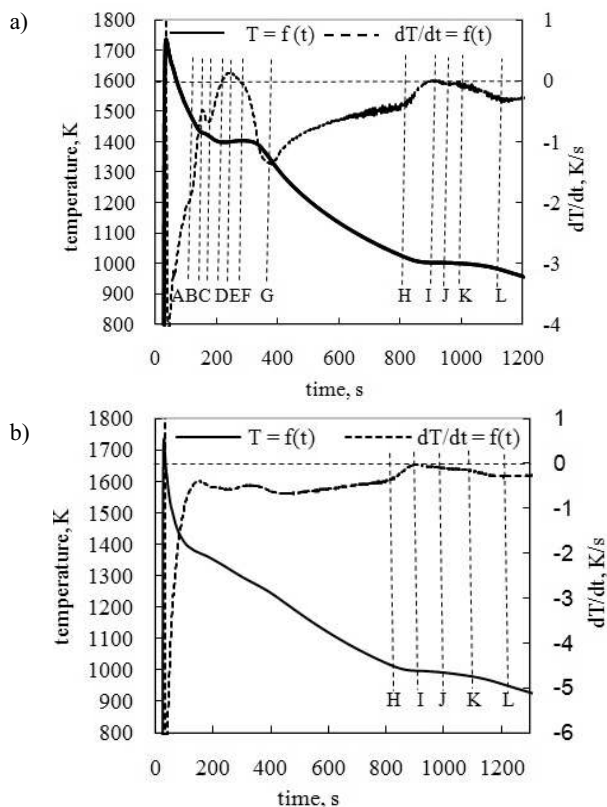


Fig. 6. DTA curves plotted for base alloy in lower part of casting body (a) and in riser (b)

Rys. 6. Krzywe TDA stopu bazowego rejestrowane w dolnej części trzonu (a) oraz nadlewie (b)

The DTA curves shown in Figure 7 (a, b) illustrate the thermal effects related to the solidification of the alloy containing the mixture of titanium and carbon placed at the mould bottom. The curves show some differences when compared to the base alloy (Fig. 6). This mainly refers to the absence of the thermal effect caused by the crystallisation of primary austenite (Fig. 7a). Another difference evident in the examined curves is the maximum temperature recorded by thermocouples, which for the base alloy is the same in the casting body (Fig. 6a) and in the riser (Fig. 6b) and amounts to 1737 K. In the case of the alloy containing the substrates of SHS reaction placed at the mould bottom, the difference in the maximum temperatures between thermocouples 1 and 2 is 85 K.

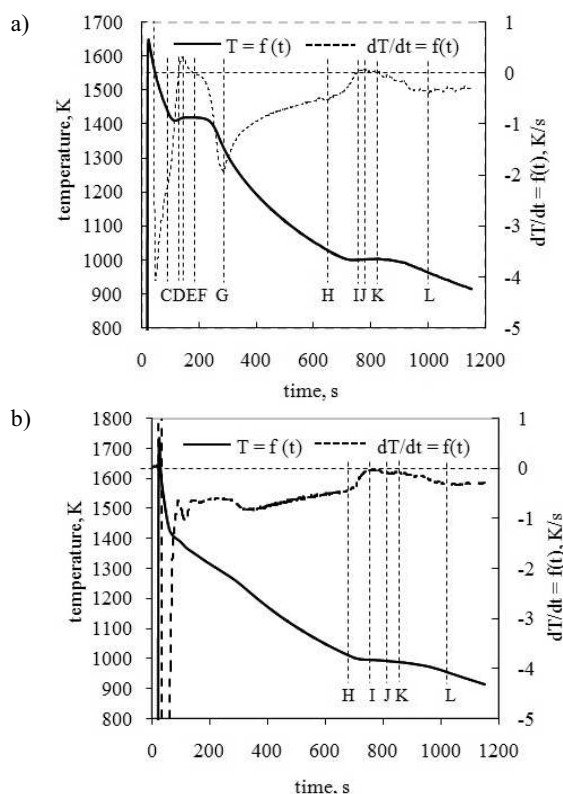


Fig. 7. DTA curves of alloy containing substrates of SHS reaction plotted for lower part of casting body (a) and riser (b)

Rys. 7. Krzywe TDA stopu zawierającego substraty reakcji SHS, rejestrowane w dolnej części trzonu odlewu (a) oraz nadlewie (b)

DISCUSSION

The structural analysis of the casting body has indicated the presence of ferrite, graphite and TiC carbides (Fig. 2), the crystallisation of which was the result of an SHS reaction occurring between the titanium and carbon powders introduced to the mould. The products of this synthesis were, after a very turbulent reaction, spontaneously dispersed over the casting surface area. The consequence was the formation in the outer part of the casting of a composite layer from 3 to 6×10^{-3} m thick (Fig. 3). The carbides distributed in this layer had the size from 2 to 10×10^{-6} m, and their

shape was close to an oval one, locally forming compact and coagulated clusters of a considerable size (Figs. 4, 5). The maximum hardness of the TiC carbides obtained by in situ synthesis was 1950 MHV.

The DTA curves obtained for the base alloy and for the alloy containing a mixture of the SHS reaction substrates placed at the bottom of the mould indicate the differences in the solidification process of both materials. This mainly refers to the solidification of the alloy containing the SHS reaction substrates, where the thermal effects caused by the crystallisation of primary austenite do not occur (Fig. 7a). These effects occur in the base alloy (Fig. 6a). The obtained results indicate a change in the alloy composition caused by the presence of titanium and carbon powders introduced to the mould. In addition, the highly exothermic reaction of the titanium carbide synthesis leads to a rise in temperature in the reaction zone. The recorded temperature difference between the riser and the lower part of the casting body containing the reaction substrates is 85 K (Fig. 7).

CONCLUSIONS

The paper presents a method to fabricate composite layers in iron castings. The main feature of this method is the possibility of synthesizing the hard TiC carbides formed in a previously selected area of casting to enhance its properties, mainly functional ones.

The main conclusions that can be drawn from the studies are:

- it is possible to obtain in an iron casting a composite layer of a thickness from 3 to 6 x 10⁻³ m, containing oval-shaped TiC carbides of hardness reaching 1950 MHV and a grain size from 2 to 10 x 10⁻⁶ m,
- the process of carbide synthesis in the melt can cause changes in the chemical composition induced by substrates introduced to the mould,
- as a result of the highly exothermic reaction, the alloy temperature rises in the reaction zone.

REFERENCES

- [1] Yisan W., Yichao D., Jing W., Fengjun Ch., Jianguo S., In situ production of vanadium carbide particulates rein-

forced iron matrix surface composite by cast-sintering, *Materials and Design* 2007, 28, 2202-2206.

- [2] Kieback A., Neubrand, H., Riedel, Processing techniques for functionally graded materials, *Materials Science and Engineering A* 2003, 362, 81-105.
- [3] Kwon H., Kang S., Microstructure and mechanical properties of TiC-WC-(Ti,W)C-Ni cermets, *Materials Science and Engineering A* 2009, 520, 75-79.
- [4] Kim J., Seo K., Kang S., Microstructure and mechanical properties of Ti-based solid-solution cermets, *Materials Science and Engineering A* 2011, 528, 2517-2521.
- [5] Jura S., Suchoń J., Compound castings of steel and cast iron, *Solidification of Metals and Alloys* 1995, 24, 67-70.
- [6] Suchoń J., Bond formation between cast iron and cast steel in bimetallic castings, *Archives of Foundry* 2006, 22, 483-489.
- [7] Jeshvaghani R.A., Shamanian M., Jaberzadeh M., Enhancement of wear resistance of ductile iron surface alloyed by stellite 6, *Materials and Design* 2011, 32, 2028-2033.
- [8] Asano K., Yoneda H., Formation of in situ composite layer on magnesium alloy surface by casting process, *Materials Transactions* 2008, 49, 10, 2394-2398.
- [9] Wang Y., Ding Y., Wang J., Cheng F., Shi J., In situ production of vanadium carbide particulates reinforced iron matrix surface composite by cast-sintering, *Materials and Design* 2007, 28, 2202-2206.
- [10] Pampuch R., Lis J., Advanced methods for SHS powders developed in Krakow, *International Journal of Self Propagating High-Temperature Synthesis* 2008, 17, 85-91.
- [11] Li Y.X., Hu J.D., Wang H.Y., Guo Z.X., Study of TiC/Ni₃Al composites by laser ignited self-propagating high-temperature synthesis (LISHS), *Chemical Engineering Journal* 2008, 140, 621-625.
- [12] Park H., Nakata K., Tomida S., In situ formation of TiC particulate composite layer on cast iron by laser alloying of thermal sprayed titanium coating, *Journal of Materials Science* 2000, 35, 747-755.
- [13] Khor K.A., Gu Y.W., Dong Z.L., Plasma spraying of functionally graded yttria stabilized zircon/NiCoCrAlY coating system using composite powder, *Journal of Thermal Spray Technology* 2000, 9, 245-249.
- [14] Merzhanov A.G., Combustion processes that synthesize materials, *Journal of Materials Processing Technology* 1996, 56, 222-241.
- [15] Fraś E., Olejnik E., Janas A., Kolbus A., FGMs generated method SHSM, *Archives of Foundry Engineering* 2009, 9, 123-128.
- [16] Fraś E., Olejnik E., Janas A., Kolbus A., Fabrication of in situ composites layer on cast steel, *Archives of Foundry Engineering* 2010, 10, 175-180.